BIOCHEMISTRY
including biophysical chemistry & molecular biology
Article

Biochemistry **2011,** *50,* 1309–1320 1309
DOI: 10.1021/bi101985j

Structure of *trans*-Resveratrol in Complex with the Cardiac Regulatory Protein Troponin C[†]

Sandra E. Pineda-Sanabria,[‡] Ian M. Robertson,[‡] and Brian D. Sykes*

Department of Biochemistry, Faculty of Medicine and Dentistry, University of Alberta, Edmonton, Alberta, Canada T6G 2H7. [‡]These authors contributed equally to this work.

Received December 13, 2010; Revised Manuscript Received January 10, 2011

ABSTRACT: Cardiac troponin, a heterotrimeric protein complex that regulates heart contraction, represents an attractive target for the development of drugs for treating heart disease. Cardiovascular diseases are one of the chief causes of morbidity and mortality worldwide. In France, however, the death rate from heart disease is remarkably low relative to fat consumption. This so-called "French paradox" has been attributed to the high level of consumption of wine in France, and the antioxidant *trans*-resveratrol is thought to be the primary basis for wine's cardioprotective nature. It has been demonstrated that *trans*-resveratrol increases the myofilament Ca^{2+} sensitivity of guinea pig myocytes [Liew, R., Stagg, M. A., MacLeod, K. T., and Collins, P. (2005) *Eur. J. Pharmacol. 519*, 1−8]; however, the specific mode of its action is unknown. In this study, the structure of *trans*-resveratrol free and bound to the calcium-binding protein, troponin C, was determined by nuclear magnetic resonance spectroscopy. The results indicate that *trans*-resveratrol undergoes a minor conformational change upon binding to the hydrophobic pocket of the C-domain of troponin C. The location occupied by *trans*-resveratrol coincides with the binding site of troponin I, troponin C's natural binding partner. This has been seen for other troponin C-targeting inotropes and implicates the modulation of the troponin C−troponin I interaction as a possible mechanism of action for *trans*-resveratrol.

The physiological function of the heart is to pump blood throughout the body to fulfill the oxygen and nutrient demands of the organism. The thin filament in heart muscle is made up of actin, tropomyosin, and troponin. Troponin is a heterotrimeric protein complex formed by the Ca^{2+}-binding subunit, troponin C (TnC);[1] the inhibitory subunit, troponin I (TnI); and the tropomyosin-binding subunit, troponin T (TnT). Cardiac TnC (cTnC) has four EF-hand metal-binding sites (I−IV), two in each of its terminal domains. The C-terminal (cCTnC) and N-terminal (cNTnC) domains are connected by a flexible linker, as shown by the NMR (*1*) and X-ray structures (*2*). In cNTnC, site I is defunct and site II is a low-affinity Ca^{2+}-binding site; on the other hand, both site III and site IV in cCTnC are functional and can bind either Mg^{2+} or Ca^{2+}. During the contraction−relaxation cycle, the cytosolic Ca^{2+} concentration dramatically oscillates: at high Ca^{2+} levels, cNTnC becomes Ca^{2+}-saturated, which primes cNTnC for binding with the "switch" region of cTnI ($cTnI_{147-163}$) (*3*, *4*); at low Ca^{2+} concentrations, Ca^{2+} dissociates from cNTnC, leading to the release of $cTnI_{147-163}$. Alternatively, cCTnC remains saturated with either Mg^{2+} or Ca^{2+} throughout the contraction cycle and is associated with the "anchoring" region of cTnI ($cTnI_{34-71}$), an interaction that may play both structural and regulatory roles (*5*). Association of $cTnI_{147-163}$ with cNTnC drags the "inhibitory" region of cTnI ($cTnI_{128-147}$) off of actin, and tropomyosin changes its orientation on the thin filament; the myosin binding site is exposed on actin, and myosin binding to actin leads to contraction (for reviews, see refs *6* and *7*).

The strength of heart muscle contraction is regulated by the amount of Ca^{2+} released from the sarcoplasmic reticulum into the cytosol and by the response of the myofilaments to Ca^{2+}. Many popular cardiotonic agents (such as digitalis or dobutamine) improve contraction in the failing heart by elevating the intracellular Ca^{2+} concentration; however, intracellular Ca^{2+} concentration modulation carries risks associated with Ca^{2+} overload such as cardiac arrhythmias, cell injury, or cell death. These limitations have shifted interest to a novel class of cardiotonic drugs, Ca^{2+} sensitizers. Ca^{2+} sensitizers induce a positive inotropic effect by modulating the myofilament's response to cytosolic Ca^{2+} and consequently may circumvent the risks associated with altering Ca^{2+} homeostasis (*8*). The essential role that cTnC plays in regulation of contraction makes it a logical target for the development of Ca^{2+} sensitizers. Several ligands that have been found to have a Ca^{2+} sensitizing ability through direct interaction with cTnC include trifluoperazine (TFP) (*9*), bepridil (*9*, *10*),

[†]This work is supported by grants from the Canadian Institutes of Health Research (FRN 37760), the National Institutes of Health (R01 HL-085234), the Heart and Stroke Foundation of Canada to B.D.S., and the Alberta Heritage Foundation for Medical Research to I.M.R. The Canadian National High Field NMR Centre is funded by the Canadian Institutes of Health Research, the Natural Science and Engineering Research Council of Canada, and the University of Alberta.

*To whom correspondence should be addressed. Phone: (780) 492-5460. Fax: (780) 492-0886. E-mail: brian.sykes@ualberta.ca.

[1]Abbreviations: NMR, nuclear magnetic resonance; ROESY, rotating frame Overhauser effect spectroscopy; NOESY, nuclear Overhauser effect spectroscopy; HSQC, heteronuclear single-quantum coherence; HMQC, heteronuclear multiple-quantum coherence; NOE, nuclear Overhauser effect; TnC, troponin C; cTnC, cardiac TnC; cCTnC, C-domain of cTnC; cNTnC, N-domain of cTnC; TnI, troponin I; cTnI, cardiac TnI; TnT, troponin T; cTnT, cardiac TnT; EGCg, epigallocatechin gallate; TFP, trifluoperazine; CSP, chemical shift perturbation; TCEP, tris(2-carboxyethyl)phosphine; SSE, sum of squared error; PDB, Protein Data Bank.

Published on Web 01/12/2011

levosimendan (*11*−*13*), and EMD 57033 (*14*−*16*). While the majority of these compounds target cNTnC to elicit their Ca^{2+} sensitizing effects, EMD 57033 functions by targeting cCTnC (*15*). In addition, the natural tea polyphenol, epigallocatechin gallate (EGCg), modulates heart muscle contractility through an interaction with cCTnC (*17*−*19*). These results suggest that both domains of cTnC represent targets for the development of Ca^{2+} sensitizers for treating heart failure.

Cardiovascular diseases are the main cause of death worldwide. Interestingly, the mortality rate from heart disease is significantly lower in France than in other countries with comparable diets rich in fat and other risk factors. It has been suggested that this so-called "French paradox" may be attributable to high levels of wine consumption in France (*20*). *trans*-Resveratrol (3,4′,5-trihydroxystilbene) is produced in grapevines after fungal infection and exposure to ultraviolet light (*21*), and Siemann and Creasy proposed that it might be the biologically active ingredient of red wine (*22*). *trans*-Resveratrol (resveratrol) has a variety of reported physiological effects, including antiplatelet aggregation, anti-inflammatory, and antioxidant activity linked to longevity (*23*, *24*); protective effects in skin photosensitivity (*25*); neurodegenerative diseases (*26*); cancer chemoprevention (*27*, *28*); and cardioprotection (*29*). Among its cardioprotective effects, resveratrol has been shown to improve the recovery of ventricular function, including developed pressure in the face of ischemia reperfusion injury (*30*). Resveratrol was shown to directly affect the contractile function of guinea pig myocytes, and it increased the level of cell shortening in half the cells tested and decreased the level of shortening in the other half. In the cells where it induced contraction, its relation with the Ca^{2+} transients was quantitatively determined, indicating an increase in myofilament Ca^{2+} sensitivity (*31*). These findings indicate a direct relation between resveratrol and the Ca^{2+}-regulated elements in myocytes; however, structural details of this interaction remain unclear.

This study investigates the interaction between cTnC and resveratrol using the structural technique NMR spectroscopy. There have been a number of research groups that describe the applications of relatively sparse NMR data for the determination of the structures of protein−ligand complexes (*32*−*35*). Recently, Hoffman and Sykes described a procedure for determining the structure of W7 bound with cNTnC using a previously determined structure of cNTnC as a template (*36*). A similar protocol was followed here, and it was discovered that resveratrol binds to cCTnC in a manner similar to that of EGCg (*19*) and EMD 57033 (*14*). Several key hydrophobic interactions between cCTnC and resveratrol stabilize the binary structure. It also appears that resveratrol undergoes an only slight conformational change upon binding cCTnC. The solution structure provides clues about the cardioprotective mechanism of resveratrol, and molecular details of the interface between resveratrol and cCTnC may aid in the design of novel cCTnC-targeting drugs.

EXPERIMENTAL PROCEDURES

Sample Preparation. Labeled [^{15}N]- and [^{15}N,^{13}C]cCTnC and [^{15}N]cTnC were obtained from *Escherichia coli* strains containing the expression vector as previously described (*37*, *38*). *trans*-Resveratrol was purchased from Sigma-Aldrich Inc. (99% pure as determined by gas chromatography). All NMR samples had volumes of 500 μL and consisted of 100 mM KCl, 10 mM imidazole or 8 mM imidazole-d_4 and 2 mM imidazole, and 0.5 mM DSS-d_6 as an NMR reference standard. Protein concentrations were ~0.2 mM for full-length cTnC and ~0.5 mM for cCTnC with 20 and 10 mM $CaCl_2$, respectively. The sample pH was maintained at ~6.9 for all NMR experiments. Although resveratrol naturally exists in *cis* and *trans* isomeric forms, *trans*-resveratrol was used in this study because of its higher concentrations in red wine (0−15 μg/mL) in contrast with that of *cis*-resveratrol (0−5 μg/mL) (*24*). Stock solutions of 20 mM *trans*-resveratrol (resveratrol) in a 100 mM tris(2-carboxyethyl)phosphine (TCEP)/DMSO-d_6 solution were prepared. TCEP was used to allay oxidation of resveratrol, which was done for EGCg and ascorbic acid (*19*, *39*). The resveratrol:cCTnC concentration ratio was ~4:1 for NMR experiments with the complex. All the stock solutions were prepared fresh prior to each experiment and were wrapped with aluminum foil to prevent photodegradation.

NMR Spectroscopy and Data Processing. The NMR data used for this study were collected on Varian Inova 500 MHz and Unity 600 MHz spectrometers at 30 °C or a Varian Inova 800 MHz spectrometer at 25 °C. All spectrometers have triple-resonance probes with Z-pulsed field gradients. One-dimensional ^{1}H and two-dimensional ^{1}H−^{1}H NOESY and ^{1}H−^{1}H ROESY experiments were performed with resveratrol in D_2O with mixing times of 100 ms for the NOESY and 50, 150, 200, and 300 ms mixing times for the ROESY experiments. Two-dimensional ^{1}H−^{13}C HSQC and ^{1}H−^{15}N HSQC experiments were conducted to monitor the titration of resveratrol into ^{13}C- and ^{15}N-labeled or ^{15}N-labeled cCTnC. Intramolecular NOEs of resveratrol when in complex with cCTnC were measured with the two-dimensional ^{13}C−^{15}N-filtered NOESY experiment with a mixing time of 100 ms (*40*, *41*); intermolecular distance restraints between resveratrol and cCTnC were derived from two-dimensional ^{13}C-edited/filtered NOESY-HSQC (mixing times of 150, 200, and 250 ms) (*42*) and three-dimensional ^{13}C-edited/filtered HMQC-NOESY (mixing times of 200 and 250 ms) (*43*, *44*) experiments. To determine whether the conformation of cCTnC was perturbed by the presence of resveratrol, a two-dimensional ^{1}H−^{1}H NOESY was conducted with the cCTnC·resveratrol complex in D_2O with a mixing time of 150 ms. VNMRJ (Varian Inc.) was used for the analysis of one-dimensional NMR spectra, and all two-dimensional and three-dimensional NMR data were processed with NMRPipe (*45*) and analyzed with NMRView (*46*). Chemical shifts of cCTnC were assigned using those deposited for cTnC (*1*), and the methionine methyls were assigned from assignments previously determined by mutagenesis (*47*). The interaction between resveratrol and cCTnC is in fast exchange, so the resonances from cCTnC could be followed throughout the titration of resveratrol and the assignments translated to the chemical shifts of the cCTnC·resveratrol complex.

Resveratrol Assignment and Assessment of Stability. The proton chemical shifts of resveratrol were assigned in D_2O by the use of one-dimensional ^{1}H, two-dimensional ^{1}H−^{1}H NOESY, and two-dimensional ^{1}H−^{1}H ROESY NMR experiments. To test the stability of resveratrol in aqueous solution, 500 μL samples of ~0.3 mM resveratrol were prepared in D_2O. ^{1}H NMR spectra were recorded in 1 h increments to test for oxidative degradation. Another sample of resveratrol was prepared with 10 mM TCEP, and the sample stability was reassessed. In both samples, the pD was ~7.0.

NMR Structure and Ab Initio Calculations of Resveratrol Free in Solution. The PRODRG web server (*48*) was used to create initial coordinates of resveratrol, and XPLO-2D (*49*) was used to generate topology and parameter files for resveratrol.

The structure of resveratrol was determined by ROE intensities of resveratrol with a mixing time of 200 ms. XPLOR-NIH (*50*) was used to calculate the solution structure of resveratrol. Four NOEs contributed to the structure calculation, which were binned from strong (2.00−1.80 Å) to medium (2.80−1.80 Å) to weak (3.60−1.80 Å). The simulated annealing comprised square-well potentials for interproton distances and a patch to keep the aromatic rings and olefin bond planar; the aromatic rings of resveratrol were allowed to freely rotate around the C1′−Cα′ and C1−Cα bonds. One hundred structures were calculated, and the 10 lowest-energy structures were kept. The lowest-energy solution structure of free resveratrol was used as an input structure in Gaussian03 (*51*) to calculate the total density and electrostatic potential (ESP). The energy calculation was performed in aqueous solvent with Becke's three-parameter Lee, Yang, Parr (B3LYP) hybrid functional with a split-valence basis set and polarization d- and p-orbitals added [B3LYP/6-311++G(d, p)]. Final contour surfaces were represented using GaussView version 3.0.

Titrations of Resveratrol into cTnC and cCTnC. The 20 mM resveratrol stock solution was titrated into an NMR tube containing full-length ^{15}N-labeled cTnC, ^{15}N-labeled cCTnC, or ^{15}N- and ^{13}C-labeled cCTnC. Resveratrol was added to final concentrations of 62, 185, 367, 665, 956, 1517, and 2050 μM for the titration with cTnC and to final concentrations of 43, 171, 379, 581, 975, 1346, and 1701 μM for the titration with cCTnC. One-dimensional ^{1}H and two-dimensional ^{1}H−^{15}N HSQC spectra were recorded at each titration point. Additionally, ^{1}H−^{13}C HSQC spectra were recorded throughout the titration of resveratrol into ^{13}C- and ^{15}N-labeled cCTnC. At each titration point, the HSQC spectra were recorded, and residue specific chemical shift perturbations (CSPs) that were well resolved and underwent a large change were kept for the dissociation constant calculation. Chemical shift changes ($\Delta\delta$) were calculated using the following equation:

$$\Delta\delta = \sqrt{(\Delta\delta_H)^2 + \frac{1}{25}(\Delta\delta_N)^2}$$

The dissociation constants (K_D) for resveratrol were calculated by using a global fitting approach with xcrvfit (www.bionmr.ualberta.ca/bds/software/xcrvfit), as described previously (*52*). Briefly, the set of kept titration curves was fit using a fixed K_D range and a floating final shift value (because residues were perturbed to a varying extent). The sum of squared error (SSE) was minimized by optimizing the K_D, and thus, a global K_D that best fit all the CSPs was calculated. The binding of resveratrol to cTnC and cCTnC was fit with a 1:1 stoichiometry:

$$\text{troponin} + \text{resveratrol} \leftrightarrow \text{troponin} \cdot \text{resveratrol}$$

Concentrations of cTnC and cCTnC were calculated by integration of the one-dimensional slice of the ^{1}H−^{15}N HSQC spectrum and comparison of the spectral intensity with that of a sample with a protein concentration determined by amino acid analysis. The concentrations of the resveratrol stock solutions were determined via comparison of the proton spectral intensity of resveratrol peaks with the DSS proton intensity. Concentrations of cTnC, cCTnC, and resveratrol were then corrected for dilution that occurred during the titrations. Because the addition of resveratrol slowly decreased the pH of the sample, the pH was adjusted to ~6.9 with 1 M NaOH when necessary.

j-Surface Mapping. Jsurf was used to localize the binding site of resveratrol on cCTnC. Jsurf approximates the origin of the CSP as a single-point dipole in the center of an aromatic ring from a ligand (*53*). With the coordinates of cTnC as input, Jsurf depicts the coordinates of a ligand ring as a dot based on the magnitude and sign of the CSPs. The region that shows the highest dot density is termed the j-surface and is the place where the aromatic constituents of a ligand are most likely to reside. The chemical shifts in the ^{1}H−^{13}C HSQC spectrum of the final point in the titration of cCTnC (CS_{PL}) with resveratrol were subtracted from the initial chemical shifts of cCTnC (CS_P).

$$CSP = CS_{PL} - CS_P$$

Only peaks that were well-resolved and underwent a concentration-dependent CSP of ≥0.012 ppm in the proton dimension were used in the analysis; results were displayed with PyMOL.

Calculation of the Structure of the cCTnC·Resveratrol Complex. The structure of the cCTnC·resveratrol complex was calculated using restraints for cCTnC from the cCTnC·EGCg complex because the CSPs induced by both ligands are quite similar. A similar datum-driven protocol has been used for the cNTnC·W7 complex (*36*). Distance restraints for cCTnC were calibrated with CYANA (*54*) using an upper limit of 6 Å. Dihedral angle restraints from TALOS (*55*) were used as well as 12 distance restraints from X-ray crystallographic data of chelating oxygen atoms to the two Ca^{2+} ions. CYANA was used to calculate 100 structures of cCTnC, of which the 30 conformers with the lowest target function were used to further refine the structure with XPLOR-NIH. The restraints were converted from CYANA format into XPLOR-NIH format. The simulated annealing protocol of XPLOR-NIH, with 10000 high-temperature steps and 6000 cooling steps, was used in the structure calculation. The NOEs were averaged using the R-6 with a soft well potential. Spin diffusion was a concern because the mixing times of 200 and 250 ms for the measurement of intermolecular NOEs were high. Therefore, only NOEs that had an NOE intensity of $\geq \mu - {}^1/_2\sigma$ were kept for the structure calculation, and all were calibrated with the same distance. A total of 23 intermolecular NOEs (6.0−1.8 Å) and four intramolecular NOEs (2.6−1.8 Å) were used in the structure calculation; 100 structures were calculated, from which the 50 lowest-energy structures were kept for refinement in explicit solvent with a water box edge length of 18.8 Å. It has been shown that refinement in explicit solvent including electrostatic potentials can improve the quality of structures (*56*). Atomic charges calculated by Gaussian03 for resveratrol (see above) were included at this point in the structure calculation. The final ensemble is represented by the 20 lowest-energy structures after water refinement and was validated by Procheck (*57*) available with the online Protein Structure Validation Software (PSVS) suite (http://psvs-1_4-dev.nesg.org/), and the structural statistics are listed in Table 1 of the Supporting Information.

RESULTS

Stability of Resveratrol. NMR chemical shift assignments of *trans*-resveratrol (resveratrol) or *trans*-resveratrol derivatives have been previously reported in acetone (*58*), chloroform (*59*), DMSO-d_6 (*60*), and a DMSO-d_6/D_2O mixture (*61*). Resveratrol (Figure 1) in D_2O was assigned by one-dimensional ^{1}H, two-dimensional ^{1}H−^{1}H NOESY, and two-dimensional ^{1}H−^{1}H ROESY NMR experiments. The aromatic protons were assigned using three- and four-bond couplings. H2′ and H6′ were distinguished from H3′ and H5′ in the two-dimensional NOESY and ROESY experiments; only H2′ and H6′ made ROE contacts with the ethylene protons (Hα and Hα′). The unambiguous

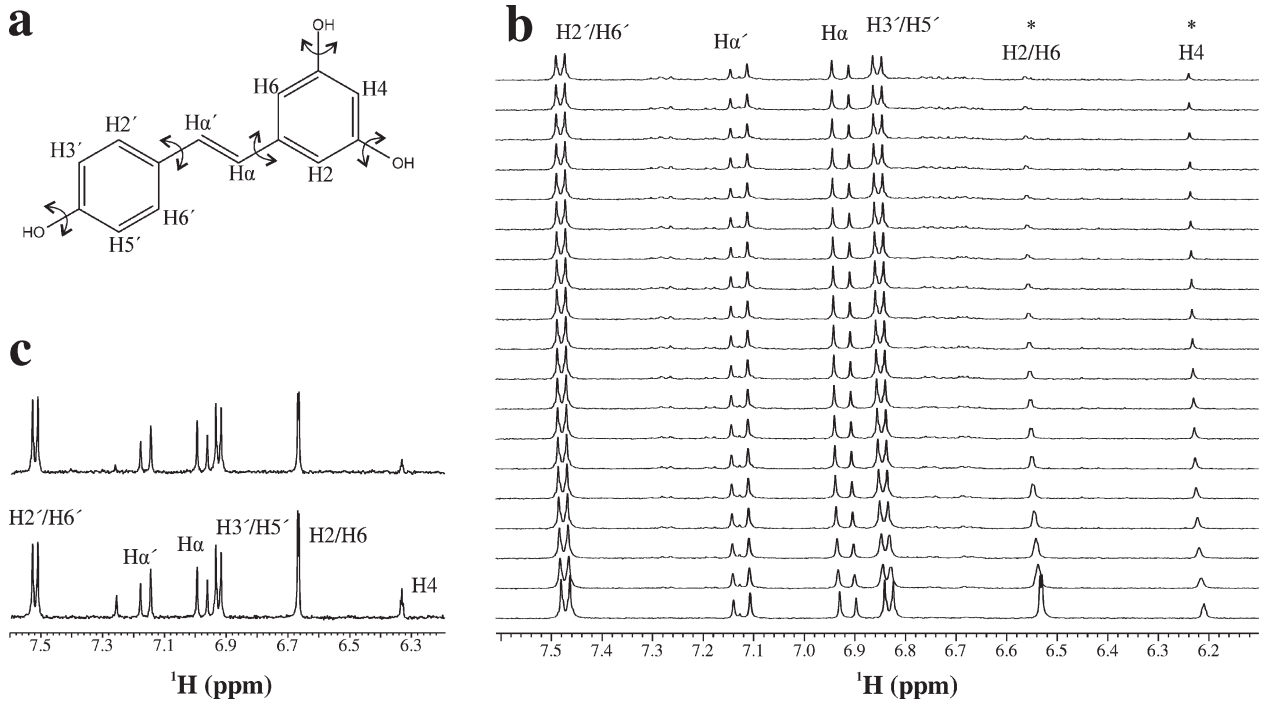

FIGURE 1: Stability of resveratrol. (a) Chemical structure of resveratrol. Torsion angles that were allowed to rotate during structure calculations are indicated. (b) Degradation of resveratrol as a function of time. One-dimensional ^{1}H NMR spectra were recorded every 1 h (bottom, first spectrum; top, last spectrum). (c) Spectrum of resveratrol in the presence of 10 mM TCEP. The bottom spectrum was recorded at time zero, and the top spectrum is that of resveratrol after 24 h. The unlabeled peak downfield from Hα′ is from [^{1}H]imidazole that exchanged with D_2O over time.

assignments of Hα and Hα′ were facilitated with previously published assignments for resveratrol (*58*−*61*). The ethylene protons had a vicinal coupling constant of 16.4 Hz, consistent with a *trans*-ethylene bond (*62*).

The stability of resveratrol has been addressed previously (*63*). The authors found that under acidic conditions, resveratrol was stable for at least 42 h, while at pH 10, resveratrol had a half-life of 1.6 h. Because three-dimensional NMR experiments require a stable sample for 2−3 days and the samples are at neutral pH, the necessity of a reducing agent was investigated. The degradation of resveratrol was measured by acquiring one-dimensional ^{1}H NMR spectra at 1 h time points. Significant degradation of resveratrol was observed, primarily in the di-*m*-hydroxyl (di-*m*-OH) ring (Figure 1b), and a half-life of 5−6 h was estimated by monitoring the chemical shift change of the H2 and H6 proton pair (Figure 1 of the Supporting Information). The sample also changed color from clear to brown over the course of 24 h. Next, 10 mM TCEP was added to a sample of resveratrol, and no significant degradation occurred after 1 day (Figure 1c). There was some decrease in peak intensities; however, there was no change in chemical shift or sample color, even after 72 h.

Structure of Resveratrol in D_2O. To determine the structure of resveratrol in solution, two-dimensional ROESY spectra were recorded with different mixing times (50, 150, 200, and 300 ms); the ROE buildup curve is shown in Figure 2 of the Supporting Information. Two slices from the ROESY spectrum (mixing time of 200 ms) are shown in Figure 2a. The H2′ and H6′ protons make much stronger ROEs with the ethylene protons than the H2 and H6 protons do (Table 1). The strong ROE between H2′ or H6′ and Hα is only consistent with a coplanar orientation of the *p*-hydroxyl (*p*-OH) ring and olefin. On the other hand, weak, approximately uniform ROEs between the ethylene protons and H2 and H6 are indicative of a roughly equal distance between H2 and H6 and Hα and Hα′, consistent with a tilted and/or flexible di-*m*-OH ring. The ensemble of the 10 lowest-energy structures is shown in Figure 2b. The Cα′−Cα−C1−C6 and Cα−Cα′−C1′−C6′ torsion angles can be used to describe the orientations of the two phenolic rings with respect to the olefin. In Table 2, the torsion angles for a number of structures of resveratrol are listed. The *p*-OH ring is coplanar (0.5 ± 0.3°) with the olefin, whereas the di-*m*-OH ring is tilted by 43.9 ± 0.4°. The structure of free resveratrol has also been determined by NMR spectroscopy in DMSO (*60*) and by X-ray crystallography (*64*); both structures revealed an overall planar structure. The X-ray structure of a trimethoxy derivative of resveratrol was less planar, particularly with respect to the orientation of the di-*m*-O-CH_3 ring (*65*). In the crystal structure of resveratrol, extensive hydrogen bonds contribute to the planarity of resveratrol, while the inability of 3,4′,5-trimethoxystilbene to form intermolecular hydrogen bonds resulted in a slight twist of the rings. It is possible that the presence of TCEP in the sample decreased the amount of intermolecular hydrogen bonding of resveratrol by perturbing stacking interactions and may explain the somewhat tilted conformation of the di-*m*-OH ring. The lowest-energy structure in the ensemble of resveratrol was used to calculate its electronic properties with the quantum chemistry program Gaussian03 (*51*) (Figure 2c).

Resveratrol Binding to cTnC. To characterize resveratrol's interaction with troponin, we titrated resveratrol into a sample containing ^{15}N-labeled cTnC. ^{1}H−^{15}N HSQC NMR spectra were recorded throughout the titration, and most of the large chemical shift perturbations (CSPs) were of backbone amides in the C-domain of cTnC (Figure 3 of the Supporting Information). In addition, the residues that typically experience large perturbations upon binding of cTnI or a ligand to the N-domain (*4*, *52*) such as Gly34, Gly42, Glu66, and Asp73 remained relatively

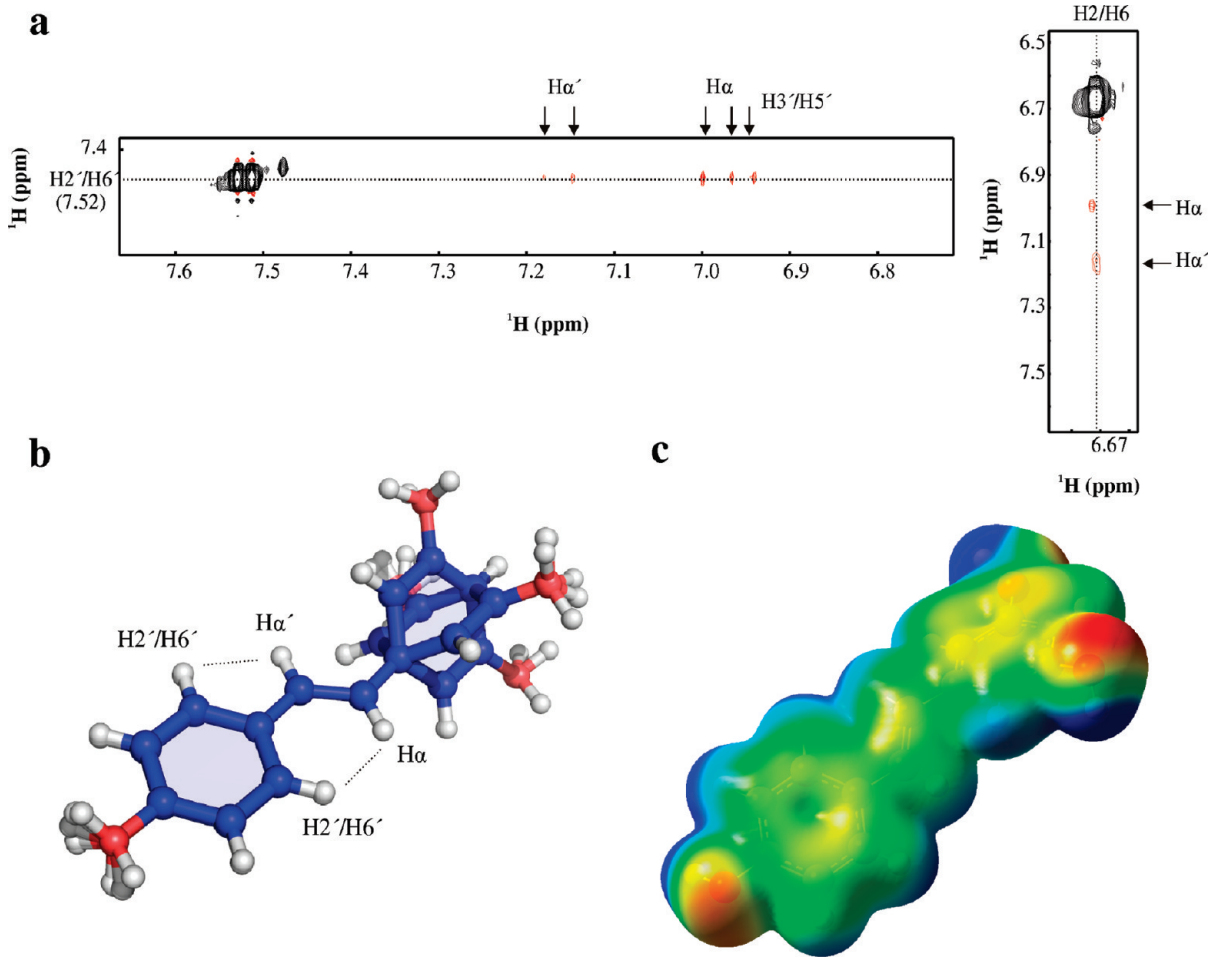

FIGURE 2: Structure of resveratrol. (a) Two-dimensional ROESY spectrum of resveratrol in D_2O. (b) Ensemble of resveratrol aligned with the olefin atoms: Hα′, Cα′, Hα, and Cα. ROEs measured between H2′/H6′ and Hα and Hα′ are drawn on the structure to illustrate that the intensity of the ROE between H2′/H6′ and Hα requires a planar orientation of the phenol ring. (c) Gaussian calculation from the lowest-energy structure of resveratrol. The electrostatic potential of resveratrol was mapped with an isovalue of 0.004 e/Å^3 (-7×10^{-2} eV, red; 7×10^2 eV, blue).

Table 1: Comparison of Relative ROE or NOE Intensities

contact	free resveratrol[a]	bound resveratrol
H2′/H6′−Hα′	0.51	0.67
H2′/H6′−Hα	1.00	0.84
H2/H6−Hα	0.17	0.71
H2/H6−Hα′	0.16	1.00

[a]With a mixing time of 200 ms.

unperturbed. The linear nature of the CSPs is indicative of a 1:1 stoichiometry for resveratrol binding to cTnC. Multiple binding would lead to nonlinear CSPs, which was observed for TFP and bepridil binding to cTnC (*9*). Using xcrvfit, the CSPs of the backbone amides of Thr124, Gly125, Ile128, Thr129, Gly140, Gly159, and Glu161 were plotted as a function of resveratrol:cTnC concentration; a global dissociation constant (K_D) of 243 μM (SSE = 0.02) was determined (Figure 3b of the Supporting Information).

Resveratrol Binding to cCTnC. To test whether the interaction between resveratrol and cTnC was the same as in the isolated C-domain, resveratrol was titrated into cCTnC. Two-dimensional ^{1}H−^{13}C and ^{1}H−^{15}N HSQC experiments were used to monitor the titration of resveratrol into a sample containing cCTnC (Figure 3a,b). The ^{1}H−^{13}C HSQC spectrum (without resveratrol) was assigned using chemical shift assignments deposited for cTnC (*1*). Because resveratrol interacts with cCTnC in fast exchange, most assigned resonances could be easily followed throughout the titration. Global dissociation constants of 240 μM (SSE = 0.08) from the backbone amides and 301 μM (SSE = 0.02) from the methyl groups of cCTnC were calculated (Figure 3). The residue specific CSPs are almost identical in both pattern and amplitude between the titrations of resveratrol with cCTnC and cTnC (Figure 3c of the Supporting Information). The comparable dissociation constants and CSP patterns suggest that resveratrol interacts with cCTnC the same as it does with full-length cTnC.

Following determination of the affinity and stoichiometry of the binding of resveratrol to cCTnC, j-surface mapping was conducted to predict resveratrol's binding location on cCTnC. j-Surface mapping works to predict a binding site by assuming that the ring current from an aromatic constituent of a ligand is the primary source of ligand-induced CSPs (*53*). Typically, amide protons are used in the calculation; however, it is well-established that cTnC undergoes a large conformational change upon ligand binding. Thus, most of the backbone CSPs are indicative of a global change in its structure rather than direct contact with a given ligand (*66*). To circumvent this difficulty, the CSPs of methyl protons were used in the j-surface calculation, as changes in these chemical shifts are more likely indicative of direct interactions with resveratrol. Methyl resonances used in the calculation were

Table 2: Comparison of Resveratrol Ring Orientation with Those of Other Structures[a]

structure	*p*-OH ring twist (deg)	di-*m*-OH ring twist (deg)
X-ray structure of resveratrol (*64*)	8.02	−2.98
X-ray structure of 3,5,4′-trimethoxystilbene (*65*)	3.53/−9.16	21.13/−16.32
NMR structure of resveratrol (D_2O)[b]	0.5 ± 0.3	43.9 ± 0.4
NMR structure of cCTnC[b]	18.6 ± 10.6	35.2 ± 8.7
X-ray structure of chalcone synthase (PDB entry 1CGZ) (*70*)	−9.21	−32.00
X-ray structure of transthyretin (PDB entry 1DVS) (*71*)	0.7/1.06	0.55/1.13
X-ray structure of quinone reductase 2 (PDB entry 1SG0) (*73*)	0.23/0.23	3.11/2.15
X-ray structure of mutant chalcone synthase (PDB entry 1U0W) (*72*)	−0.16/−2.98	0.18/−1.49
X-ray structure of stilbene synthase (PDB entry 1Z1F) (*74*)	62.92	−66.97
X-ray structure of cytosolic sulfotransferase (PDB entry 3CKL)	19.84/20.51	5.80/19.16
X-ray structure of leukotriene A4 hydrolase (PDB entry 3FTS) (*76*)	−27.28	−17.65
X-ray structure of F_1-ATPase (PDB entry 1JIZ) (*75*)[c]	27.68/19.90/−35.06/42.25	−9.25/7.60/45.69/−21.39

[a]Ring twist illustrates the orientation of the ring with comparison to the central olefin of resveratrol. The *p*-OH ring twist is the Cα−Cα′−C1′−C6′ torsion angle; the di-*m*-OH ring twist is the Cα′−Cα−C1−C6 torsion angle. For the NMR structures, both positive and negative torsions were measured so they are reported in absolute degrees. Multiple values are given when more than one resveratrol is present in the X-ray structures. [b]From this study. [c]The authors could not distinguish between two binding modes and therefore concluded that resveratrol may bind to F_1-ATPase in multiple poses.

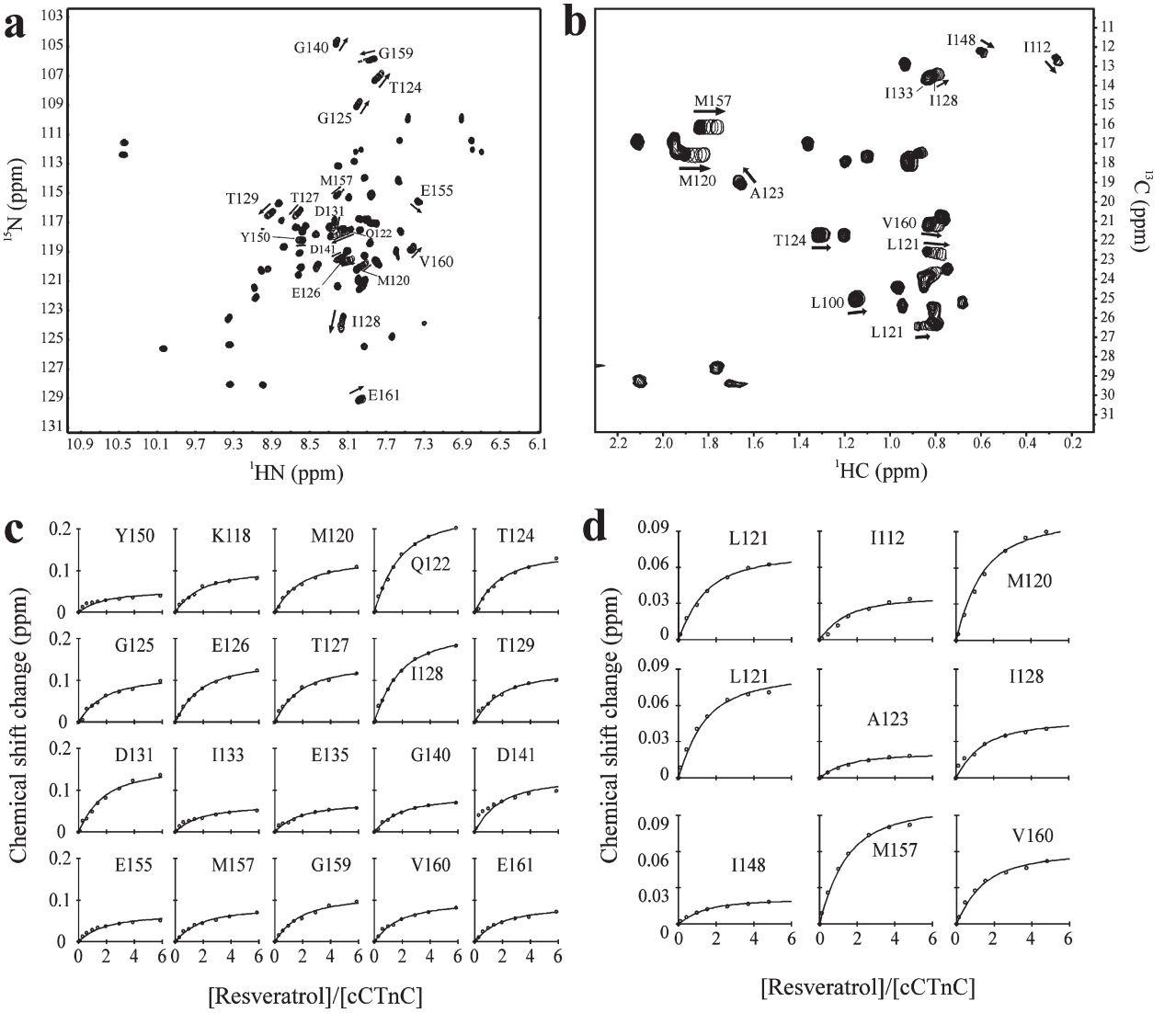

FIGURE 3: Binding of resveratrol to cCTnC. (a) $^{1}H-^{15}N$ HSQC and (b) $^{1}H-^{13}C$ HSQC (methyl region) spectra of cCTnC recorded throughout the titration with resveratrol. The first point in the titration is represented with all 20 contours, whereas each titration point with resveratrol is represented by a single contour. Directions of CSPs are denoted with arrows for several peaks. Fitting of (c) $^{1}H-^{15}N$ HSQC and (d) $^{1}H-^{13}C$ HSQC NMR data with xcrvfit to determine the dissociation constant.

those that underwent a ≥|0.012| ppm change in the proton dimension. These included Ile112, Met120, Leu121, Ala123, Ile128, Ile148, Met157, and Val160. The structure of cTnC (PDB entry 1aj4) (*1*) was used in the j-surface calculation, and the results localize

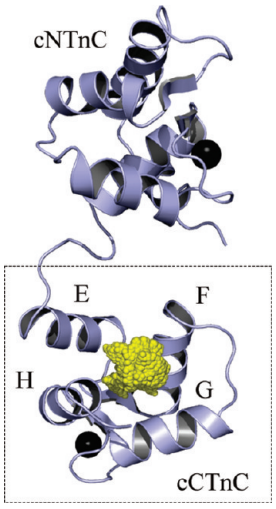

FIGURE 4: j-Surface representation. Results are mapped on the structure of cTnC (PDB entry 1aj4). The backbone atoms are depicted in cartoon representation (light blue); Ca^{2+} ions are represented by black spheres, and the j-surface dot density is depicted using yellow spheres. Residues used in the j-surface calculation were Leu121, Val160, Ala123, Ile148, Ile128, Met157, Met120, and Ile112.

the binding of resveratrol to the cleft formed by the four helices of cCTnC (Figure 4). There appear to be two j-surfaces: one near the surface of cCTnC and the other deeper in the core. Because the j-surface calculation is unable to identify the specific pose resveratrol adopts when bound to cCTnC, NMR spectroscopy was used to identify intermolecular contacts between resveratrol and cCTnC.

Structure of the cCTnC·Resveratrol Complex. The structure of cCTnC free or in complex with a number of binding partners has been determined by both X-ray crystallography and NMR spectroscopy (*1*, *2*, *14*, *19*, *67*−*69*). Instead of determining the structure of cCTnC again, we pursued a datum-driven docking approach. The $^{1}H-^{15}N$ HSQC CSPs induced by resveratrol were compared with those induced by ligands that interact with cCTnC: $cTnI_{34-71}$, EMD 57033, and EGCg (Figure 4 of the Supporting Information). The CSPs are most similar between resveratrol and EGCg (in both magnitude and pattern); hence, the intramolecular NOEs and dihedral restraints of cCTnC used in the structure calculation were taken from the cCTnC·EGCg complex (*19*). The only new restraints used in the structure calculation were those that defined the structure and pose of resveratrol in complex with cCTnC.

Intermolecular NOEs were measured between cCTnC and resveratrol with ^{13}C- and ^{15}N-edited/filtered NOESY experiments. These experiments measure solely NOEs between a ^{13}C- and ^{15}N-labeled molecule and an unlabeled molecule. Two-dimensional ^{13}C- and ^{15}N-filtered/edited NOESY HSQC (*42*) experiments were conducted with mixing times of 150, 200, and 250 ms to establish the optimal mixing times for the three-dimensional experiments. Because most of the intermolecular contacts observed were between methyl groups from cCTnC and the aromatic ring protons of resveratrol, the three-dimensional ^{13}C-edited/filtered HMQC NOESY experiment (*43*, *44*) was conducted. This NMR experiment is optimized for the identification of intermolecular NOEs involving ^{13}C-labeled methyls (*44*). Two three-dimensional ^{13}C-edited/filtered HMQC NOESY experiments were conducted: one with a mixing time of 250 ms and one with a mixing time of 200 ms. Intermolecular NOEs that had intensities of ≥0.04 were included in the structure calculation. This is because of the long experimental mixing times of the intermolecular NOESY experiments, and the tightly coupled nature of resveratrol increased the likelihood of spin diffusion. When all NOEs were included in the structure run, many violations occurred, presumably because of spin diffusion. The intermolecular NOEs from a mixing time of 200 ms used in the structure calculation are shown in Figure 5a. Initially, a structure calculation followed, similar to what was done for the EGCg calculation. The quality of the structure was subsequently improved by conducting a structure refinement in water; at this stage, electrostatic potentials and atomic charges were included (*56*). The 20 lowest-energy structures of the complex are shown in panels b and c of Figure 5. The structure indicates that, congruent with the prediction by j-surface mapping, resveratrol is localized to the hydrophobic pocket of cCTnC. The resveratrol−-cCTnC interaction site is populated primarily by nonpolar contacts. Resveratrol contacts the side chains of Leu100, Leu117, Leu121, Thr124, Leu136, Met157, and Val160 (Figure 5d). Weak NOEs between resveratrol and Ile148 and Ile112 (both β-sheet residues), not used in the structure run because they did not meet the intensity cutoff criteria, were also consistent with the final structure. In addition to the methyl−resveratrol contacts, the structure indicates that arene−arene contacts formed between resveratrol and Phe104, Phe153, and Phe156 contribute to the binding energy of resveratrol.

In addition to measuring intermolecular NOEs between resveratrol and cCTnC to determine their relative positions, we also determined the conformation of bound resveratrol. The intramolecular NOEs of resveratrol were measured with the ^{13}C- and ^{15}N-filtered NOESY experiment (*40*, *41*), which works by removing signals from a ^{13}C- and ^{15}N-labeled molecule and keeping only signals from an unlabeled molecule. All structure-defining intramolecular NOEs were close to the same intensity, with the strongest being the H2/H6−Hα′ contact (see Table 1 and Figure 5 of the Supporting Information). This is in contrast with the case for free resveratrol, in which the strongest ROE was between H2′/H6′ and Hα, and suggests that resveratrol undergoes a slight conformational change upon binding cCTnC. To limit bias in the structure of resveratrol during the calculation, one distance (2.6−1.8 Å) for the four intramolecular contacts was used, and the final structure was checked against the raw NOE data. Indeed, the results are consistent with the relative NOE intensities: the closest proton pair was the H2/H6−Hα′ proton pair (2.24 ± 0.14 Å). The other distances are as follows: H2/H6−Hα, 2.57 ± 0.05 Å; H2′/H6′−Hα′, 2.28 ± 0.06 Å; and H2′/H6′−Hα, 2.32 ± 0.07 Å. The torsion angles were measured for resveratrol in complex with cCTnC and were compared to those determined for free resveratrol. The *p*-OH ring is more twisted (18.6 ± 10.6°) than in free resveratrol (from 0.5 ± 0.3°), whereas the torsion angle of the di-*m*-OH ring is not significantly different (43.9 ± 0.4° vs 35.2 ± 8.7°).

There have been a number of crystal structures of resveratrol in complex with proteins determined, including alfalfa chalcone synthase (CHS) (*70*), the fibril-forming transthyretin (TTR) (*71*), a variant of alfalfa CHS (*72*), quinone reductase 2 (QR2) (*73*), peanut stilbene synthase (STS) (*74*), bovine F1-ATPase (*75*), leukotriene A4 hydrolase (*76*), and human cytosolic sulfotransferase (not published; but deposited as PDB entry 3ckl). In most of these structures, resveratrol is planar or slightly distorted from a planar conformation with torsion angles of ≤45°; the only exception is in the peanut STS·resveratrol complex, in which

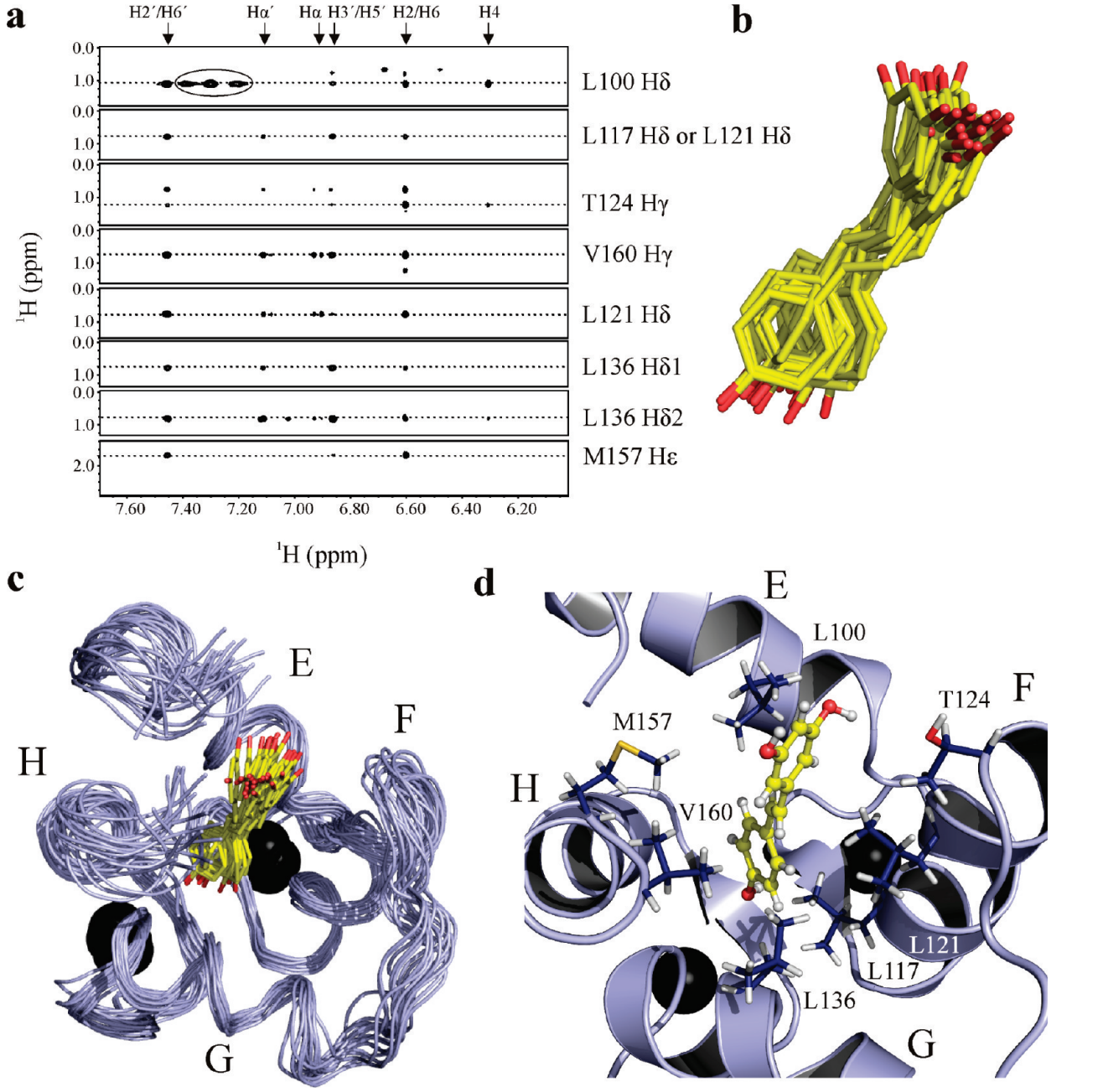

FIGURE 5: Structure of the cCTnC·resveratrol binary complex. (a) Strip plots showing the NOEs between resveratrol and cCTnC. The resveratrol assignments are at the top of the spectrum; cCTnC assignments are indicated at the right. Peaks that are circled represent intramolecular cCTnC NOEs that were not adequately filtered. (b) Ensemble of resveratrol from the binary complex. The carbon atoms are colored yellow and the oxygen atoms red. (c) Twenty lowest-energy structures of the cCTnC·resveratrol complex with the backbone trace of cCTnC colored light blue and helices E−H labeled. (d) Resveratrol's binding pocket on the lowest-energy structure of cCTnC. Residues for which NOEs were measured are labeled and depicted as sticks with carbon atoms colored dark blue; resveratrol is shown in ball-and-stick representation (hydrogen atoms colored white). Calcium ions are shown as black spheres.

both rings of resveratrol are twisted > 60° (*74*) (see Table 2). These results, in conjunction with the structures of free resveratrol and resveratrol derivatives, point to a relatively rigid resveratrol framework. In accordance with the X-ray and NMR structures, Caruso et al. calculated single-point energy versus the torsion angle of the *p*-OH ring and found the lowest-energy structure is a planar conformation (*64*).

The structure of cCTnC in the cCTnC·resveratrol complex is not much different from that of cCTnC in other complexes. The Cα atoms from residues in secondary structure elements of the cCTnC·resveratrol complex were superimposed with those of cCTnC (PDB entry 3ctn), the cCTnC·EMD 57033 complex (PDB entry 1ih0), the cCTnC·EGCg complex (PDB entry 2kdh), and the cCTnC·cTnI$_{34-71}$ complex (PDB entry 1j2d), and root-mean-square deviations of 1.17, 1.50, 1.02, and 1.26 Å, respectively, were determined. These values indicate that resveratrol does not significantly perturb the structure of cCTnC. Helix E of the cCTnC·resveratrol complex is shifted away from the hydrophobic cleft, like that of the cCTnC·EMD5033 complex. The position of helix F of the cCTnC·resveratrol complex is in a position almost identical to that in the cCTnC·EGCg and cCTnC·cTnI$_{34-71}$ complexes; however, it is shifted farther from helix E of cCTnC and not as far as in the cCTnC·EMD 57033 complex.

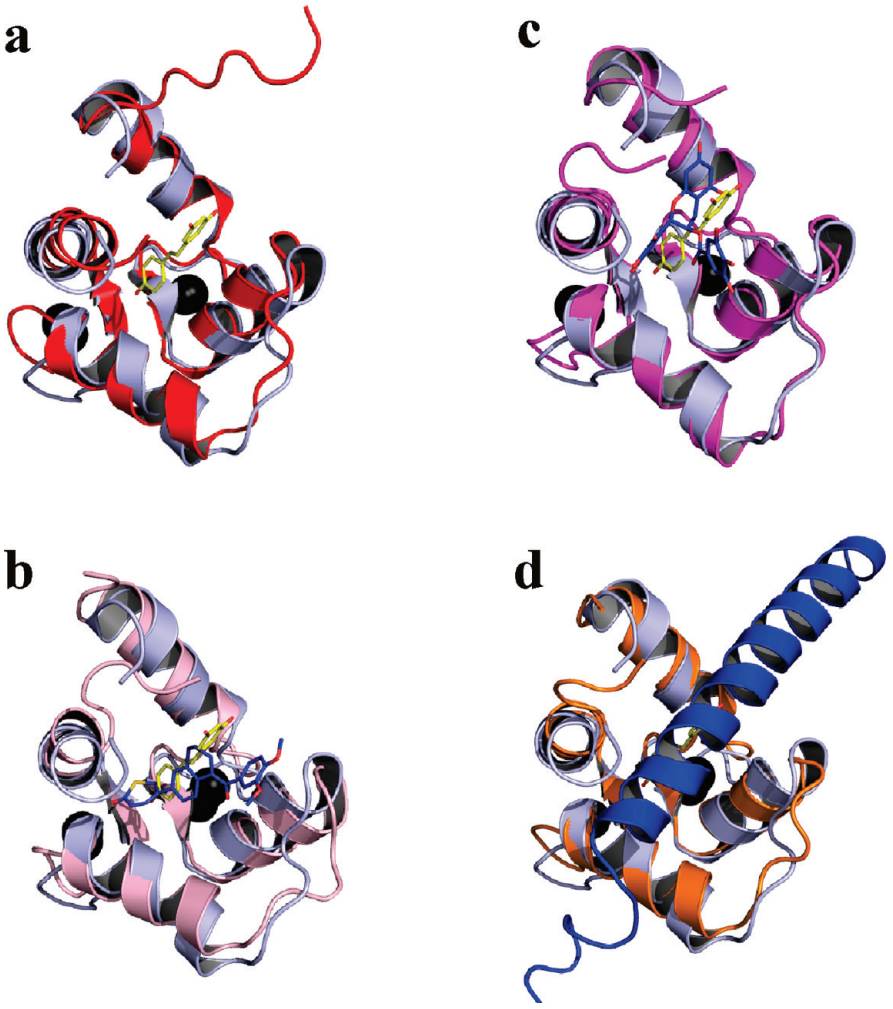

FIGURE 6: Structural comparisons. Superimposition of the cCTnC·resveratrol complex (light blue) and (a) cCTnC (red, PDB entry 3ctn), (b) the cCTnC·EMD 57033 complex (pink, PDB entry 1ih0), (c) the cCTnC·EGCg complex (magenta, PDB entry 2kdh), and (d) the cCTnC·$cTnI_{34-71}$ complex (orange, PDB entry 1j1d). The carbon atoms for resveratrol are colored yellow, and the oxygen atoms are colored red. For the other structures, ligand carbon atoms are colored blue, oxygen atoms red, nitrogen atoms dark blue, and sulfur atoms yellow. Ca^{2+} ions are shown as black spheres.

DISCUSSION

The regulatory role of the Ca^{2+}-dependent interaction between $cTnI_{147-163}$ and cNTnC is well-established and has been the primary interaction site on which the development of Ca^{2+} sensitizers focused (*77*, *78*). However, the exclusive development of drugs that target cNTnC has been scrutinized as a growing body of evidence indicates that cCTnC is also involved in contraction regulation. The dilated cardiomyopathy mutation of cCTnC, Gly159Asp, decreases myofilament Ca^{2+} sensitivity (*79*) via its modulation of the $cTnI_{34-71}$−cCTnC interaction (*67*). The hypertrophic cardiomyopathy mutation, Asp145Glu, increases Ca^{2+} sensitivity (*80*), presumably by weakening the binding of Ca^{2+} and cTnI to cCTnC (*81*). The ablation of the Ca^{2+} binding ability of the C-domain of cTnC increases the Ca^{2+} sensitivity of muscle contraction (*82*). There are two isoforms of TnC in insect flight muscle: the F1 isoform that regulates stretch-activated force and the F2 isoform that is responsible for Ca^{2+}-activated contraction. Although it is not clear how F1 regulates stretch activation, the interaction between the C-domain of F1 and TnH (an ortholog of cTnI) may play a role (*83*). Finally, as previously mentioned, the cardiotonic agents EMD 57033 (*15*, *84*) and EGCg (*17*, *18*) target cCTnC to modulate heart muscle contractility.

In this study, resveratrol was found to interact with the C-domain of cTnC, and the structure was determined by NMR spectroscopy. The *p*-OH group of resveratrol lies in the hydrophobic core of cCTnC, whereas the di-*m*-OH ring points toward the exterior of the protein. The stabilizing contacts between resveratrol and cCTnC are predominantly hydrophobic. In the other resveratrol·protein complexes, the binding site of resveratrol is also dominated by hydrophobic interactions; however, unlike the structure of the cCTnC·resveratrol complex, hydrogen bonds between the hydroxyls of resveratrol and the amino acids that line the binding pockets also contribute to the binding energy (*70*−*76*). The design of resveratrol with the *p*-OH group converted to a hydrophobic constituent may therefore increase its affinity for cCTnC; for example, converting the hydroxyl to a fluorine atom would increase the lipophilicity of resveratrol without dramatically decreasing its size (*85*, *86*). On the other hand, removing the *p*-OH group would undoubtedly weaken the antioxidant ability of resveratrol, especially given the fact that the *p*-OH group has been implicated as being the principal hydroxyl responsible for resveratrol's antioxidant nature (*64*, *87*−*89*).

The comparison of the structure of the cCTnC·resveratrol complex with the structures of the cCTnC·EMD 57033 and cCTnC·EGCg complexes yields insights into several key functional

groups. In the structure, the *p*-OH aromatic ring of resveratrol is positioned in a manner similar to that of the thiadiazinone ring of EMD 57033, with the *p*-hydroxyl pointed toward the cleft formed by helices G and H. The di-*m*-OH ring of resveratrol faces away from the hydrophobic cavity of cCTnC, much like the benzenediol of EGCg, which leaves its hydroxyl moieties free to form hydrogen bonds with the surrounding aqueous milieu. Therefore, the binding pose of resveratrol has features that uniquely resemble the structures of EGCg and EMD 57033 when bound to cCTnC. Resveratrol, EMD 57033, and EGCg all share their binding sites with the natural binding partner of cCTnC, $cTnI_{34-71}$ (Figure 6), and as a result may have a common mode of action. The troponin-dependent Ca^{2+} sensitizing ability of EMD 57033 has been suggested to involve a competition between EMD 57033 and $cTnI_{34-71}$ for cCTnC (*90*). The perturbation of the $cTnI_{34-71}$−cCTnC interaction may lead to an increase in the affinity of $cTnI_{128-147}$ for cTnC and thus a decrease in the level of inhibition of contraction.

It was determined that resveratrol bound to cTnC and cCTnC with micromolar affinity. This relatively low affinity of resveratrol for cTnC was anticipated, because an overly high affinity would lead to a marked increase in Ca^{2+} sensitivity. This dramatic increase in Ca^{2+} sensitivity over the long term could lead to negative effects, such as hypertrophic cardiomyopathy. On the other hand, it may be useful to optimize the resveratrol−cCTnC interaction for the development of drugs for treating acute heart failure. One method for the analysis of whether a small molecule represents a good lead molecule is to determine its ligand efficiency (LE) (*91*−*93*). LE is described by the ratio of the free energy of binding to the number of heavy atoms in a compound and is based on the premise that as a drug is optimized, it often increases in molecular weight, a trend fraught with problems, including a decrease in bioavailability through insolubility and membrane permeability (*94*).

The free energy (ΔG) of binding is

$$\Delta G = -RT \ln K_D$$

and the ligand efficiency (binding energy per non-hydrogen atom) (LE) is

$$LE = \Delta G/N$$

For resveratrol binding to cCTnC, a K_D of 240 μM has a binding energy of 4.97 kcal/mol. Resveratrol has 17 non-hydrogen atoms (14 carbon atoms and three oxygen atoms), so its ligand efficiency is 0.29 kcal/mol. This ligand efficiency corresponds to a compound with 33 non-hydrogen atoms (approximately twice the size of resveratrol, MW of 450) with a binding constant of 0.1 μM. The reasonably good ligand efficiency of resveratrol suggests that the substitution or addition of a few atoms that enhance its affinity for cCTnC may lead to novel therapies for the treatment of heart failure.

CONCLUSION

Resveratrol is a natural product found in wine that modulates the Ca^{2+} sensitivity of myofilaments (*31*). In this study, the structure of resveratrol in complex with the cardiac regulatory protein troponin C was determined by NMR spectroscopy. Consistent with the small molecules EGCg and EMD 57033, resveratrol targeted the C-domain of troponin C. The binding of resveratrol is primarily stabilized by hydrophobic contacts such as methyl−arene and arene−arene interactions. In addition to providing clues about the cardioprotective nature of resveratrol, the structure highlights several functional groups that could be modified to optimize the binding efficacy of resveratrol. Recently, the polyphenol, propyl gallate, has also been identified to act as a Ca^{2+} sensitizer (*95*), which alongside the functional and structural data for EGCg and resveratrol, points to a common mechanism by which these natural compounds target the thin filament to protect against heart failure.

ACKNOWLEDGMENT

We thank Dr. G. Moyna for making the source code for Jsurf available and for helpful instructions for its use, Drs. Monica Li and Marta Oleszczuk for insightful discussions about drug−troponin C interactions, and Dr. Pascal Mercier and Olivier Julien for helpful advice on structure calculation. We also thank David Corson and Melissa Crane for protein expression and purification and Robert Boyko for spectrometer maintenance and in-house software development. We finally thank the Canadian National High Field NMR Centre for their assistance and use of the facilities.

SUPPORTING INFORMATION AVAILABLE

Data illustrating the oxidation rate of resveratrol, resveratrol ROE intensities versus mixing time, binding of resveratrol to cTnC, ligand-dependent chemical shift perturbations of cCTnC, intramolecular NOEs of resveratrol in complex with cCTnC, and structural statistics for the ensemble of structures of the cCTnC·resveratrol complex. This material is available free of charge via the Internet at http://pubs.acs.org.

REFERENCES

1. Sia, S. K., Li, M. X., Spyracopoulos, L., Gagne, S. M., Liu, W., Putkey, J. A., and Sykes, B. D. (1997) Structure of cardiac muscle troponin C unexpectedly reveals a closed regulatory domain. *J. Biol. Chem. 272*, 18216–18221.
2. Takeda, S., Yamashita, A., Maeda, K., and Maeda, Y. (2003) Structure of the core domain of human cardiac troponin in the Ca^{2+}-saturated form. *Nature 424*, 35–41.
3. Spyracopoulos, L., Li, M. X., Sia, S. K., Gagne, S. M., Chandra, M., Solaro, R. J., and Sykes, B. D. (1997) Calcium-induced structural transition in the regulatory domain of human cardiac troponin C. *Biochemistry 36*, 12138–12146.
4. Li, M. X., Spyracopoulos, L., and Sykes, B. D. (1999) Binding of cardiac troponin-I147−163 induces a structural opening in human cardiac troponin-C. *Biochemistry 38*, 8289–8298.
5. Tripet, B., Van Eyk, J. E., and Hodges, R. S. (1997) Mapping of a second actin-tropomyosin and a second troponin C binding site within the C terminus of troponin I, and their importance in the Ca^{2+}-dependent regulation of muscle contraction. *J. Mol. Biol. 271*, 728–750.
6. Li, M. X., Wang, X., and Sykes, B. D. (2004) Structural based insights into the role of troponin in cardiac muscle pathophysiology. *J. Muscle Res. Cell Motil. 25*, 559–579.
7. Kobayashi, T., Jin, L., and de Tombe, P. P. (2008) Cardiac thin filament regulation. *Pfluegers Arch. 457*, 37–46.
8. Endoh, M. (2001) Mechanism of action of Ca^{2+} sensitizers: Update 2001. *Cardiovasc. Drugs Ther. 15*, 397–403.
9. Kleerekoper, Q., Liu, W., Choi, D., and Putkey, J. A. (1998) Identification of binding sites for bepridil and trifluoperazine on cardiac troponin C. *J. Biol. Chem. 273*, 8153–8160.
10. Li, Y., Love, M. L., Putkey, J. A., and Cohen, C. (2000) Bepridil opens the regulatory N-terminal lobe of cardiac troponin C. *Proc. Natl. Acad. Sci. U.S.A. 97*, 5140–5145.
11. Haikala, H., Kaivola, J., Nissinen, E., Wall, P., Levijoki, J., and Linden, I. B. (1995) Cardiac Troponin-C as a Target Protein for a Novel Calcium Sensitizing Drug, Levosimendan. *J. Mol. Cell. Cardiol. 27*, 1859–1866.
12. Haikala, H., Nissinen, E., Etemadzadeh, E., Levijoki, J., and Linden, I. B. (1995) Troponin C-Mediated Calcium Sensitization Induced by

Levosimendan Does Not Impair Relaxation. *J. Cardiovasc. Pharmacol. 25*, 794–801.
13. Haikala, H., Nissinen, E., Etemadzadeh, E., Linden, I. B., and Pohto, P. (1992) Levosimendan Increases Calcium Sensitivity without Enhancing Myosin Atpase Activity and Impairing Relaxation. *J. Mol. Cell. Cardiol. 24*, S97.
14. Wang, X., Li, M. X., Spyracopoulos, L., Beier, N., Chandra, M., Solaro, R. J., and Sykes, B. D. (2001) Structure of the C-domain of human cardiac troponin C in complex with the Ca^{2+} sensitizing drug EMD 57033. *J. Biol. Chem. 276*, 25456–25466.
15. Pan, B. S., and Johnson, R. G. (1996) Interaction of cardiotonic thiadiazinone derivatives with cardiac troponin C. *J. Biol. Chem. 271*, 817–823.
16. Kleerekoper, Q., and Putkey, J. A. (1999) Drug binding to cardiac troponin C. *J. Biol. Chem. 274*, 23932–23939.
17. Liou, Y. M., Kuo, S. C., and Hsieh, S. R. (2008) Differential effects of a green tea-derived polyphenol (−)-epigallocatechin-3-gallate on the acidosis-induced decrease in the Ca^{2+} sensitivity of cardiac and skeletal muscle. *Pfluegers Arch. 456*, 787–800.
18. Tadano, N., Du, C. K., Yumoto, F., Morimoto, S., Ohta, M., Xie, M. F., Nagata, K., Zhan, D. Y., Lu, Q. W., Miwa, Y., Takahashi-Yanaga, F., Tanokura, M., Ohtsuki, I., and Sasaguri, T. (2010) Biological actions of green tea catechins on cardiac troponin C. *Br. J. Pharmacol. 161*, 1034–1043.
19. Robertson, I. M., Li, M. X., and Sykes, B. D. (2009) Solution Structure of Human Cardiac Troponin C in Complex with the Green Tea Polyphenol, (−)-Epigallocatechin 3-Gallate. *J. Biol. Chem. 284*, 23012–23023.
20. Renaud, S., and Delorgeril, M. (1992) Wine, Alcohol, Platelets, and the French Paradox for Coronary Heart Disease. *Lancet 339*, 1523–1526.
21. Langcake, P., and Pryce, R. J. (1976) Production of Resveratrol by Vitis-Vinifera and Other Members of Vitaceae as a Response to Infection or Injury. *Physiol. Plant Pathol. 9*, 77–86.
22. Siemann, E. H., and Creasy, L. L. (1992) Concentration of the Phytoalexin Resveratrol in Wine. *Am. J. Enol. Vitic. 43*, 49–52.
23. Das, D. K., Mukherjee, S., and Ray, D. (2010) Resveratrol and red wine, healthy heart and longevity. *Heart Failure Rev. 15*, 467–477.
24. Lekli, I., Ray, D., and Das, D. K. (2010) Longevity nutrients resveratrol, wines and grapes. *Genes Nutr. 5*, 55–60.
25. Nichols, J. A., and Katiyar, S. K. (2010) Skin photoprotection by natural polyphenols: Anti-inflammatory, antioxidant and DNA repair mechanisms. *Arch. Dermatol. Res. 302*, 71–83.
26. Sun, A. Y., Wang, Q., Simonyi, A., and Sun, G. Y. (2010) Resveratrol as a Therapeutic Agent for Neurodegenerative Diseases. *Mol. Neurobiol. 41*, 375–383.
27. Jang, M. S., Cai, E. N., Udeani, G. O., Slowing, K. V., Thomas, C. F., Beecher, C. W. W., Fong, H. H. S., Farnsworth, N. R., Kinghorn, A. D., Mehta, R. G., Moon, R. C., and Pezzuto, J. M. (1997) Cancer chemopreventive activity of resveratrol, a natural product derived from grapes. *Science 275*, 218–220.
28. Holme, A. L., and Pervaiz, S. (2007) Resveratrol in cell fate decisions. *J. Bioenerg. Biomembr. 39*, 59–63.
29. Das, D. K., and Maulik, N. (2006) Red wine and heart: A cardioprotective journey from grape to resveratrol. *Alcohol.: Clin. Exp. Res. 30*, 84a.
30. Ray, P. S., Maulik, G., Cordis, G. A., Bertelli, A. A. E., Bertelli, A., and Das, D. K. (1999) The red wine antioxidant resveratrol protects isolated rat hearts from ischemia reperfusion injury. *Free Radical Biol. Med. 27*, 160–169.
31. Liew, R., Stagg, M. A., MacLeod, K. T., and Collins, P. (2005) The red wine polyphenol, resveratrol, exerts acute direct actions on guinea-pig ventricular myocytes. *Eur. J. Pharmacol. 519*, 1–8.
32. Bertini, I., Fragai, M., Giachetti, A., Luchinat, C., Maletta, M., Parigi, G., and Yeo, K. J. (2005) Combining in silico tools and NMR data to validate protein-ligand structural models: Application to matrix metalloproteinases. *J. Med. Chem. 48*, 7544–7559.
33. Cioffi, M., Hunter, C. A., Packer, M. J., and Spitaleri, A. (2008) Determination of protein-ligand binding modes using complexation-induced changes in H-1 NMR chemical shift. *J. Med. Chem. 51*, 2512–2517.
34. Krishnamoorthy, J., Yu, V. C. K., and Mok, Y. K. (2010) Auto-FACE: An NMR Based Binding Site Mapping Program for Fast Chemical Exchange Protein-Ligand Systems. *PLoS One 5*, No. e8943.
35. Pintacuda, G., John, M., Su, X. C., and Otting, G. (2007) NMR structure determination of protein-ligand complexes by lanthanide labeling. *Acc. Chem. Res. 40*, 206–212.
36. Hoffman, R. M. B., and Sykes, B. D. (2009) Structure of the Inhibitor W7 Bound to the Regulatory Domain of Cardiac Troponin C. *Biochemistry 48*, 5541–5552.
37. Chandra, M., Dong, W. J., Pan, B. S., Cheung, H. C., and Solaro, R. J. (1997) Effects of protein kinase A phosphorylation on signaling between cardiac troponin I and the N-terminal domain of cardiac troponin C. *Biochemistry 36*, 13305–13311.
38. Li, M. X., Gagne, S. M., Tsuda, S., Kay, C. M., Smillie, L. B., and Sykes, B. D. (1995) Calcium-Binding to the Regulatory N-Domain of Skeletal-Muscle Troponin-C Occurs in a Stepwise Manner. *Biochemistry 34*, 8330–8340.
39. Lykkesfeldt, J. (2000) Determination of ascorbic acid and dehydroascorbic acid in biological samples by high-performance liquid chromatography using subtraction methods: Reliable reduction with tris[2-carboxyethyl] phosphine hydrochloride. *Anal. Biochem. 282*, 89–93.
40. Gemmecker, G., Olejniczak, E. T., and Fesik, S. W. (1992) An Improved Method for Selectively Observing Protons Attached to C-12 in the Presence of H-1-C-13 Spin Pairs. *J. Magn. Reson. 96*, 199–204.
41. Ikura, M., and Bax, A. (1992) Isotope-Filtered 2D NMR of a Protein Peptide Complex: Study of a Skeletal-Muscle Myosin Light Chain Kinase Fragment Bound to Calmodulin. *J. Am. Chem. Soc. 114*, 2433–2440.
42. Stuart, A. C., Borzilleri, K. A., Withka, J. M., and Palmer, A. G. (1999) Compensating for variations in H-1-C-13 scalar coupling constants in isotope-filtered NMR experiments. *J. Am. Chem. Soc. 121*, 5346–5347.
43. Lee, W., Revington, M. J., Arrowsmith, C., and Kay, L. E. (1994) A Pulsed-Field Gradient Isotope-Filtered 3D C-13 HMQC-NOESY Experiment for Extracting Intermolecular NOE Contacts in Molecular Complexes. *FEBS Lett. 350*, 87–90.
44. Robertson, I. M., Spyracopoulos, L., and Sykes, B. D. (2009) The Evaluation of Isotope Editing and Filtering for Protein-Ligand Interaction Elucidation by NMR. *Biophysics and the Challenges of Emerging Threats,* 101–119.
45. Delaglio, F., Grzesiek, S., Vuister, G. W., Zhu, G., Pfeifer, J., and Bax, A. (1995) Nmrpipe: A Multidimensional Spectral Processing System Based on Unix Pipes. *J. Biomol. NMR 6*, 277–293.
46. Johnson, B. A., and Blevins, R. A. (1994) Nmr View: A Computer Program for the Visualization and Analysis of NMR Data. *J. Biomol. NMR 4*, 603–614.
47. Lin, X., Krudy, G. A., Howarth, J., Brito, R. M. M., Rosevear, P. R., and Putkey, J. A. (1994) Assignment and Calcium-Dependence of Methionyl ε-C and ε-H Resonances in Cardiac Troponin-C. *Biochemistry 33*, 14434–14442.
48. Schuttelkopf, A. W., and van Aalten, D. M. F. (2004) PRODRG: A tool for high-throughput crystallography of protein-ligand complexes. *Acta Crystallogr. D60*, 1355–1363.
49. Kleywegt, G. J., Zou, J. Y., Kjeldgaard, M., Jones, T. A., and Around, O. (2001) International Tables for Crystallography, Volume F. Crystallography of Biological Macromolecules (Rossmann, M. G., and Arnold, E., Eds.) pp 353−356, 366−367, Kluwer Academic Publishers, Dordrecht, The Netherlands.
50. Schwieters, C. D., Kuszewski, J. J., Tjandra, N., and Clore, G. M. (2003) The Xplor-NIH NMR molecular structure determination package. *J. Magn. Reson. 160*, 65–73.
51. Frisch, M. J., Trucks, G. W., Schlegel, H. B., Scuseria, G. E., Robb, M. A., Cheeseman, J. R., Montgomery, J. A., Jr., Vreven, T., Kudin, K. N., Burant, J. C., Millam, J. M., Iyengar, S. S., Tomasi, J., Barone, V., Mennucci, B., Cossi, M., Scalmani, G., Rega, N., Petersson, G. A., Nakatsuji, H., Hada, M., Ehara, M., Toyota, K., Fukuda, R., Hasegawa, J., Ishida, M., Nakajima, T., Honda, Y., Kitao, O., Nakai, H., Klene, M., Li, X., Knox, J. E., Hratchian, H. P., Cross, J. B., Bakken, V., Adamo, C., Jaramillo, J., Gomperts, R., Stratmann, R. E., Yazyev, O., Austin, A. J., Cammi, R., Pomelli, C., Ochterski, J. W., Ayala, P. Y., Morokuma, K., Voth, G. A., Salvador, P., Dannenberg, J. J., Zakrzewski, V. G., Dapprich, S., Daniels, A. D., Strain, M. C., Farkas, O., Malick, D. K., Rabuck, A. D., Raghavachari, K., Foresman, J. B., Ortiz, J. V., Cui, Q., Baboul, A. G., Clifford, S., Cioslowski, J., Stefanov, B. B., Liu, G., Liashenko, A., Piskorz, P., Komaromi, I., Martin, R. L., Fox, D. J., Keith, T., Al-Laham, M. A., Peng, C. Y., Nanayakkara, A., Challacombe, M., Gill, P. M. W., Johnson, B., Chen, W., Wong, M. W., Gonzalez, C., and Pople, J. A. (2004) Gaussian 03, Gaussian, Inc., Wallingford, CT.
52. Hoffman, R. M. B., Li, M. X., and Sykes, B. D. (2005) The binding of W7, an inhibitor of striated muscle contraction, to cardiac troponin C. *Biochemistry 44*, 15750–15759.
53. McCoy, M. A., and Wyss, D. F. (2002) Spatial localization of ligand binding sites from electron current density surfaces calculated from NMR chemical shift perturbations. *J. Am. Chem. Soc. 124*, 11758–11763.

54. Guntert, P. (2004) Automated NMR structure calculation with CYANA. *Methods Mol. Biol. 278*, 353–378.
55. Cornilescu, G., Delaglio, F., and Bax, A. (1999) Protein backbone angle restraints from searching a database for chemical shift and sequence homology. *J. Biomol. NMR 13*, 289–302.
56. Linge, J. P., Williams, M. A., Spronk, C. A. E. M., Bonvin, A. M. J. J., and Nilges, M. (2003) Refinement of protein structures in explicit solvent. *Proteins: Struct., Funct., Bioinf. 50*, 496–506.
57. Laskowski, R. A., Rullmann, J. A. C., MacArthur, M. W., Kaptein, R., and Thornton, J. M. (1996) AQUA and PROCHECK-NMR: Programs for checking the quality of protein structures solved by NMR. *J. Biomol. NMR 8*, 477–486.
58. Jayatilake, G. S., Jayasuriya, H., Lee, E. S., Koonchanok, N. M., Geahlen, R. L., Ashendel, C. L., Mclaughlin, J. L., and Chang, C. J. (1993) Kinase Inhibitors from Polygonum-Cuspidatum. *J. Nat. Prod. 56*, 1805–1810.
59. Koh, D., Park, K. H., Jung, J., Yang, H., Mok, K. H., and Lim, Y. (2001) Complete assignment of the H-1 and C-13 NMR spectra of resveratrol derivatives. *Magn. Reson. Chem. 39*, 768–770.
60. Commodari, F., Khiat, A., Ibrahimi, S., Brizius, A. R., and Kalkstein, N. (2005) Comparison of the phytoestrogen trans-resveratrol (3,4′,5-trihydroxystilbene) structures from X-ray diffraction and solution NMR. *Magn. Reson. Chem. 43*, 567–572.
61. Bonechi, C., Martini, S., Magnani, A., and Rossi, C. (2008) Stacking interaction study of trans-resveratrol (trans-3,5,4′-trihydroxystilbene) in solution by nuclear magnetic resonance and Fourier transform infrared spectroscopy. *Magn. Reson. Chem. 46*, 625–629.
62. Karplus, M. (1959) Contact Electron-Spin Coupling of Nuclear Magnetic Moments. *J. Chem. Phys. 30*, 11–15.
63. Trela, B. C., and Waterhouse, A. L. (1996) Resveratrol: Isomeric molar absorptivities and stability. *J. Agric. Food Chem. 44*, 1253–1257.
64. Caruso, F., Tanski, J., Villegas-Estrada, A., and Rossi, M. (2004) Structural basis for antioxidant activity of trans-resveratrol: Ab initio calculations and crystal and molecular structure. *J. Agric. Food Chem. 52*, 7279–7285.
65. Yin, Q., Shi, Y. M., Liu, H. M., Li, C. B., and Zhang, W. Q. (2002) (E)-3,5,4′-Trimethoxystilbene. *Acta Crystallogr. E58*, O1180–O1181.
66. Robertson, I. M., Pineda-Sanabria, S., and Sykes, B. D. (2011) Approaches to protein-ligand structure determination by NMR spectroscopy: Applications in drug binding to the cardiac regulatory protein troponin C. *Biophysics and Structure to Counter Threats and Challenges* (in press).
67. Baryshnikova, O. K., Robertson, I. M., Mercier, P., and Sykes, B. D. (2008) Dilated cardiomyopathy G159D mutation in cardiac troponin C weakens the anchoring interaction with troponin I. *Biochemistry 47*, 10950–10960.
68. Gasmi-Seabrook, G. M., Howarth, J. W., Finley, N., Abusamhadneh, E., Gaponenko, V., Brito, R. M., Solaro, R. J., and Rosevear, P. R. (1999) Solution structures of the C-terminal domain of cardiac troponin C free and bound to the N-terminal domain of cardiac troponin I. *Biochemistry 38*, 8313–8322.
69. Lindhout, D. A., and Sykes, B. D. (2003) Structure and dynamics of the C-domain of human cardiac troponin C in complex with the inhibitory region of human cardiac troponin I. *J. Biol. Chem. 278*, 27024–27034.
70. Ferrer, J. L., Jez, J. M., Bowman, M. E., Dixon, R. A., and Noel, J. P. (1999) Structure of chalcone synthase and the molecular basis of plant polyketide biosynthesis. *Nat. Struct. Biol. 6*, 775–784.
71. Klabunde, T., Petrassi, H. M., Oza, V. B., Raman, P., Kelly, J. W., and Sacchettini, J. C. (2000) Rational design of potent human transthyretin amyloid disease inhibitors. *Nat. Struct. Biol. 7*, 312–321.
72. Austin, M. B., Bowman, M. E., Ferrer, J. L., Schroder, J., and Noel, J. P. (2004) An aldol switch discovered in stilbene synthases mediates cyclization specificity of type III polyketide synthases. *Chem. Biol. 11*, 1179–1194.
73. Buryanovskyy, L., Fu, Y., Boyd, M., Ma, Y. L., Hsieh, T. C., Wu, J. M., and Zhang, Z. T. (2004) Crystal structure of quinone reductase 2 in complex with resveratrol. *Biochemistry 43*, 11417–11426.
74. Shomura, Y., Torayama, I., Suh, D. Y., Xiang, T., Kita, A., Sankawa, U., and Miki, K. (2005) Crystal structure of stilbene synthase from *Arachis hypogaea*. *Proteins: Struct., Funct., Bioinf. 60*, 803–806.
75. Gledhill, J. R., Montgomery, M. G., Leslie, A. G. W., and Walker, J. E. (2007) Mechanism of inhibition of bovine F-1-ATPase by resveratrol and related polyphenols. *Proc. Natl. Acad. Sci. U.S.A. 104*, 13632–13637.
76. Davies, D. R., Mamat, B., Magnusson, O. T., Christensen, J., Haraldsson, M. H., Mishra, R., Pease, B., Hansen, E., Singh, J., Zembower, D., Kim, H., Kiselyov, A. S., Burgin, A. B., Gurney, M. E., and Stewart, L. J. (2009) Discovery of Leukotriene A4 Hydrolase Inhibitors Using Metabolomics Biased Fragment Crystallography. *J. Med. Chem. 52*, 4694–4715 [Erratum (2010) *Biochemistry 53*, 2330−2331].
77. Li, M. X., Robertson, I. M., and Sykes, B. D. (2008) Interaction of cardiac troponin with cardiotonic drugs: A structural perspective. *Biochem. Biophys. Res. Commun. 369*, 88–99.
78. Sorsa, T., Pollesello, P., and Solaro, R. J. (2004) The contractile apparatus as a target for drugs against heart failure: Interaction of levosimendan, a calcium sensitiser, with cardiac troponin c. *Mol. Cell. Biochem. 266*, 87–107.
79. Mirza, M., Marston, S., Willott, R., Ashley, C., Mogensen, J., McKenna, W., Robinson, P., Redwood, C., and Watkins, H. (2005) Dilated cardiomyopathy mutations in three thin filament regulatory proteins result in a common functional phenotype. *J. Biol. Chem. 280*, 28498–28506.
80. Landstrom, A. P., Parvatiyar, M. S., Pinto, J. R., Marquardt, M. L., Bos, J. M., Tester, D. J., Ornmen, S. R., Potter, J. D., and Ackerman, M. J. (2008) Molecular and functional characterization of novel hypertrophic cardiomyopathy susceptibility mutations in TNNC1-encoded troponin C. *J. Mol. Cell. Cardiol. 45*, 281–288.
81. Swindle, N., and Tikunova, S. B. (2010) Hypertrophic Cardiomyopathy-Linked Mutation D145E Drastically Alters Calcium Binding by the C-Domain of Cardiac Troponin C. *Biochemistry 49*, 4813–4820.
82. Szczesna, D., Guzman, G., Miller, T., Zhao, J. J., Farokhi, K., Ellemberger, H., and Potter, J. D. (1996) The role of the four Ca^{2+} binding sites of troponin C in the regulation of skeletal muscle contraction. *J. Biol. Chem. 271*, 8381–8386.
83. Agianian, B., Krzic, U., Qiu, F., Linke, W. A., Leonard, K., and Bullard, B. (2004) A troponin switch that regulates muscle contraction by stretch instead of calcium. *EMBO J. 23*, 772–779.
84. Solaro, R. J., Gambassi, G., Warshaw, D. M., Keller, M. R., Spurgeon, H. A., Beier, N., and Lakatta, E. G. (1993) Stereoselective Actions of Thiadiazinones on Canine Cardiac Myocytes and Myofilaments. *Circ. Res. 73*, 981–990.
85. Biffinger, J. C., Kim, H. W., and DiMagno, S. G. (2004) The polar hydrophobicity of fluorinated compounds. *ChemBioChem 5*, 622–627.
86. Smart, B. E. (2001) Fluorine substituent effects (on bioactivity). *J. Fluorine Chem. 109*, 3–11.
87. Cao, H., Pan, X. L., Li, C., Zhou, C., Deng, F. Y., and Li, T. H. (2003) Density functional theory calculations for resveratrol. *Bioorg. Med. Chem. Lett. 13*, 1869–1871.
88. Del Nero, J., and De Melo, C. P. (2003) Investigation of the excited states of resveratrol and related molecules. *Int. J. Quantum Chem. 95*, 213–218.
89. Leopoldini, M., Marino, T., Russo, N., and Toscano, M. (2004) Antioxidant properties of phenolic compounds: H-atom versus electron transfer mechanism. *J. Phys. Chem. A 108*, 4916–4922.
90. Li, M. X., Spyracopoulos, L., Beier, N., Putkey, J. A., and Sykes, B. D. (2000) Interaction of cardiac troponin C with Ca^{2+} sensitizer EMD 57033 and cardiac troponin I inhibitory peptide. *Biochemistry 39*, 8782–8790.
91. Andrews, P. R., Craik, D. J., and Martin, J. L. (1984) Functional-Group Contributions to Drug Receptor Interactions. *J. Med. Chem. 27*, 1648–1657.
92. Hopkins, A. L., Groom, C. R., and Alex, A. (2004) Ligand efficiency: A useful metric for lead selection. *Drug Discovery Today 9*, 430–431.
93. Kuntz, I. D., Chen, K., Sharp, K. A., and Kollman, P. A. (1999) The maximal affinity of ligands. *Proc. Natl. Acad. Sci. U.S.A. 96*, 9997–10002.
94. Lipinski, C. A., Lombardo, F., Dominy, B. W., and Feeney, P. J. (1997) Experimental and computational approaches to estimate solubility and permeability in drug discovery and development settings. *Adv. Drug Delivery Rev. 23*, 3–25.
95. Tadano, N., Morimoto, S., Takahashi-Yanaga, F., Miwa, Y., Ohtsuki, I., and Sasaguri, T. (2009) Propyl Gallate, a Strong Antioxidant, Increases the Ca^{2+} Sensitivity of Cardiac Myofilament. *J. Pharmacol. Sci. 109*, 456–458.